Journal of Saudi Chemical Society (2017) **21**, 708–712

King Saud University

Journal of Saudi Chemical Society

www.ksu.edu.sa
www.sciencedirect.com

ORIGINAL ARTICLE

Surface-reconstructed Cu electrode *via* a facile electrochemical anodization-reduction process for low overpotential CO_2 reduction

Shixiong Min [a,b,c], Xiulin Yang [a], Ang-Yu Lu [a], Chien-Chih Tseng [a], M.N. Hedhili [a], Zhiping Lai [a,*], Lain-Jong Li [a,*], Kuo-Wei Huang [a,b,*]

[a] *Division of Physical Sciences and Engineering, King Abdullah University of Science and Technology, Thuwal 23955-6900, Saudi Arabia*
[b] *KAUST Catalysis Center, King Abdullah University of Science and Technology, Thuwal 23955-6900, Saudi Arabia*
[c] *School of Chemistry and Chemical Engineering, Beifang University of Nationalities, Yinchuan 750021, China*

Received 16 December 2016; revised 23 February 2017; accepted 12 March 2017
Available online 21 March 2017

KEYWORDS

CO_2 reduction;
Cu electrode;
High-surface-area;
High selectivity

Abstract A high-surface-area Cu electrode, fabricated by a simple electrochemical anodization-reduction method, exhibits high activity and selectivity for CO_2 reduction at low overpotential in 0.1 M $KHCO_3$ solution. A faradaic efficiency of 37% for HCOOH and 27% for CO production was achieved with the current density of 1.5 mA cm^{-2} at −0.64 V *vs.* RHE, much higher than that of polycrystalline Cu. The enhanced catalytic performance is a result of the formation of the high electrochemical active surface area and high density of preferred low-index facets.

1. Introduction

Several metal electrocatalysts have demonstrated sufficient capability for CO_2 reduction in aqueous solutions [1]. Among them, Cu has been identified to catalyze the electroreduction of CO_2 to hydrocarbons [2–4], although high overpotentials are in general required with poor selectivity. Various strategies have been attempted to improve the catalytic performance of Cu including the control of macrostructure [5], particle size [6], exposed surface facets [7], and the formation of alloys with secondary metals [8], but the selective CO_2 reduction at low overpotential remains a huge challenge. A novel strategy was recently developed by Kanan et al. to produce a nanostructured Cu electrode from its oxides [9,10], which shows a Faradic efficiency of 40% toward CO at −0.5 V *vs.* RHE, with a total current density of 2.7 mA/cm^2 [9]. However, a high temperature and a long reaction time (500 °C for 8–12 h) are typically required for the preparation of above oxide-derived Cu (OD-Cu) catalysts. There is still a continuing need for easily accessible Cu catalysts for CO_2 reduction in an energy- and

* Corresponding authors at: Division of Physical Sciences and Engineering, King Abdullah University of Science and Technology, Thuwal 23955-6900, Saudi Arabia (K.-W. Huang).
E-mail addresses: zhiping.lai@kaust.edu.sa (Z. Lai), lance.li@kaust.edu.sa (L.-J. Li), hkw@kaust.edu.sa (K.-W. Huang).
Peer review under responsibility of King Saud University.

ELSEVIER Production and hosting by Elsevier

http://dx.doi.org/10.1016/j.jscs.2017.03.003
1319-6103

time-efficient manner. It has been reported that the electrochemical oxidation and reduction is an effective method to prepare high active Ag electrocatalysts for CO_2 reduction [11,12]. Since Cu has an extensive redox electrochemistry based on oxidation to Cu^{2+} and reduction to Cu^{1+} and Cu^0 [13,14], it is highly desirable to explore the Cu electrochemistry to generate efficient catalysts for the CO_2 reduction reaction by a solution-based method. Herein, we report the preparation of a Cu electrocatalyst with a high-surface area for efficient CO_2 reduction *via* a facile anodization-reduction process.

2. Experimental

For the preparation of highly dense $Cu(OH)_2$ nanowires (NWs) on Cu foil substrate, pieces of Cu foil ($1.5 \times 1.0\ cm^2$) were first washed with 1 M HCl solution for several seconds to remove the native oxide layer. After that, Cu foil was electrochemically anodized in 1 M NaOH solution at a current density of 2 mA cm^{-2} in a three-electrode system with a Pt foil ($2.0 \times 1.0\ cm^2$) and a saturated Ag/AgCl used as counter and reference electrode, respectively. The morphologies of samples were observed by an FEI Quanta 600 Scanning Electron Microscope (SEM) and an FEI Titan ST Transmission electron microscopy (TEM). The X-ray diffraction (XRD) patterns were recorded on a Bruker model D8 Advance. X-ray photoelectron spectroscopy (XPS) was conducted using a Kratos Axis Ultra DLD spectrometer. All the electrochemical experiments were carried out with a Biologic VMP-300 potentiostat in an air-tight and glass frit-separated two compartment three-electrode electrochemical cell. For the bulk electrolysis of CO_2, the cathodic compartment of the cell was degassed and saturated with CO_2 at a rate of 10 mL min^{-1}. The eluent was delivered directly to the sampling loop of an on-line gas chromatograph (Agilent 7890B). The liquid product HCOOH was analyzed using a high-pressured liquid chromatography (HPLC, Agilent technologies) system.

3. Results and discussion

SEM image (Fig. 1(a)) of a Cu electrode anodized at 12 min showed that the anodized Cu foil was entirely covered by nanowires with diameters in the range of 100–250 nm and an average length of 4 μm. XRD and XPS analysis revealed that the product was dominated by $Cu(OH)_2$ and Cu phases (Fig. 1 (e) and (f)) [15], indicating that the growth of $Cu(OH)_2$ NWs on the surface of Cu foil. During the course of our study, a two-step synthesis of $Cu(OH)_2$ and CuO nanowire arrays on Cu foil and the electrochemical CO_2 reduction were also reported with the focus on hydrocarbon formation. [16] TEM image of the products (Fig. 1(b)) clearly indicated their nanowire structure with a thickness smaller than 10 nm, while the SAED pattern gave their [1 0 0] orientation. High-resolution TEM (HRTEM) image (Fig. S1(a)) showed the formation of plentiful cavities on $Cu(OH)_2$ NWs. The density and average length of $Cu(OH)_2$ NWs can be easily controlled by adjusting the anodization time. The XRD patterns in Fig. S2 showed that the intensity for the characteristic peaks of Cu $(OH)_2$ increased sustainably with the anodization time while the SEM images (Fig. S3) indicated that the length of NWs increased linearly from ~1.75 to 7.0 μm as the anodization time increased.

High-surface-area Cu electrodes were then obtained by subsequently reducing the as-prepared $Cu(OH)_2$ NWs under the CO_2 reduction conditions (denoted as "anodized Cu" hereafter). Anodized Cu electrode exhibited a flower-like structure with aggregated nanoparticles formed on the tips of the wires (Fig. 1(c) and (d)), a direct result of the surface reconstruction. The HRTEM image in Fig. S1(b) also clearly indicated the formation of grain-boundaries between the nanocrystals, similar to the Cu electrode derived from Cu oxides [9]. XRD patterns and XPS spectrum collected after the electrochemical reduction only provided peaks of metallic Cu, suggesting that the Cu^0 surface was responsible for the following observed activity for CO_2 reduction.

The polycrystalline Cu (poly-Cu) electrode exhibited poor CO (1.5%) and HCOOH (9%) selectivity with almost 90% FE for H_2 evolution (Fig. 1(g)) at applied potential of -0.64 V *vs.* RHE. In contrast, CO and HCOOH selectivities on the anodized Cu electrodes were enhanced, while the H_2 FE was suppressed. Specifically, the CO selectivity continued to increase with the anodization time from 2 min up to 12 min, while the HCOOH selectivity initially increased and reached a plateau of 34–38% FE beyond 8 min. The total FE for CO (27%) + HCOOH (37%) reached a maximum value of 64% at 12 min, where the H_2 FE was below 40%. Meanwhile, the anodized Cu electrodes showed a higher catalytic geometric current density (j_{gcd}) for the CO_2 reduction as compared to poly-Cu and the j_{gcd} increased rapidly with the anodization time and reached a maximum at 8 min (2.5 mA cm^{-2}), and then became constant in the range of 10–16 min (1.4–1.8 mA cm^{-2}) (Fig. S4). Since the anodized Cu electrode possesses nanostructured surfaces, the clearly enhanced j_{gcd} and FE could be ascribed to the increased number of catalytically active sites. The electrochemically active surface (ECSA) of anodized Cu electrodes determined by measuring the double-layer capacitance (Fig. S5 and Table S1) is one order of magnitude higher than that of poly-Cu and increased linearly with the anodization time, supporting the positive correlation between j_{gcd} and FE and active sites (Fig. S6).

The anodized Cu electrode was also identified to selectively reduce CO_2 at lower overpotentials. Notably, the anodized Cu exhibited appreciable CO (~9%) and HCOOH (~5%) production started at ~−0.3 V *vs.* RHE (Fig. 2(a)), while poly-Cu was totally inert at this potential. When anodized Cu electrode was polarized to more negative potentials, the FEs for CO and HCOOH could be enhanced obviously and a peak FE for HCOOH and CO is obtained at −0.64 V *vs.* RHE. It has been noted that the formation of higher hydrocarbons can be detected on both poly-Cu and anodized Cu electrodes at much negative applied potentials. More specifically, total FEs of 11.3 and 33.1% for CH_4 and C_2H_4 production were obtained the on poly-Cu electrode at −0.941 and −0.996 V *vs.* RHE, respectively, whereas the anodized Cu electrode produces trace C_2H_4 at all the applied potentials. These results are consistent with the previous observations on the Cu_2O-derived Cu catalyst [9], indicating that the surface structures of Cu $(OH)_2$-derived Cu catalyst though a electro anodization-reduction route are distinct from those of the polycrystalline Cu. On the other hand, the anodized Cu electrode has higher j_{gcd} than the poly-Cu electrode in the potential range of −0.3 to −1.0 V *vs.* RHE (Fig. 2(b)), which is associated to its high surface area.

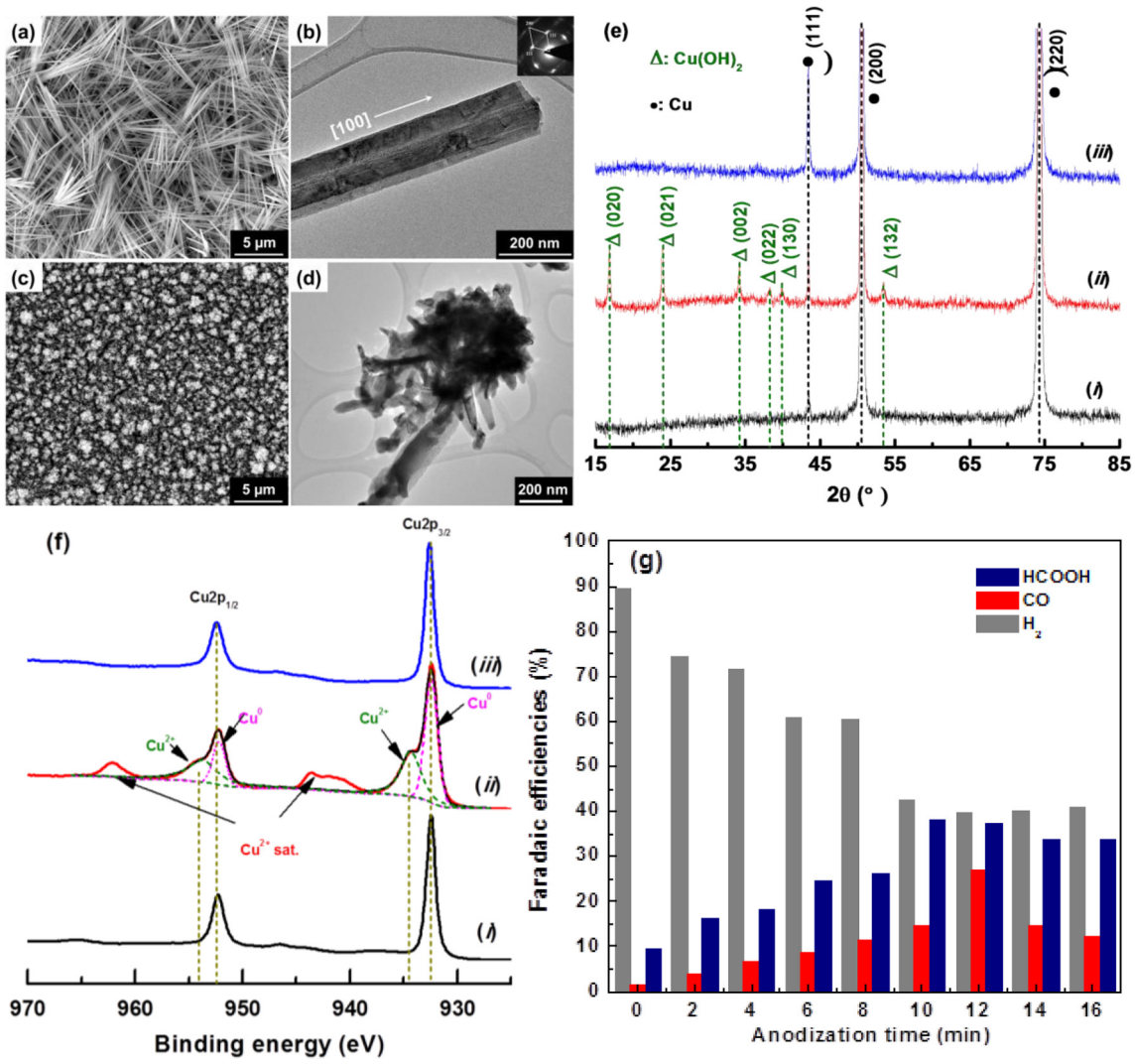

Fig. 1 SEM, TEM images of anodized Cu electrode (12 min) (a,b) and the same electrode after CO_2 reduction electrolysis at −0.64 V *vs.* RHE (c,d). (f) XRD patterns and (f) XPS spectra of the poly-Cu (*i*), the anodized Cu electrode (12 min) (*ii*), and the anodized Cu electrode after electrochemical reduction in CO_2-saturated 0.1 M $KHCO_3$ solution at −0.64 V *vs.* RHE (*iii*). (g) FEs of H_2, CO, and HCOOH for poly-Cu and those anodized at different times in CO_2-saturated 0.1 M $KHCO_3$ at −0.64 V *vs.* RHE (with experimental errors of 5–10%).

In order to get kinetic insights into the enhanced CO_2 reduction efficiency on the anodized Cu electrode, the partial current density for each major product was plotted against applied potentials (Fig. S7(a) and (d)). Although the H_2 FE on anodized Cu electrode decreased significantly in the potential range of −0.3 to −0.75 V *vs.* RHE, the partial current densities for H_2 formation were relatively constant, indicating that the increase in the CO_2 reduction selectivity was not due to the decrease in the H_2 evolution rate, but the more rapidly increasing production rates of HCOOH and CO. In comparison, the H_2 formation rate dominated over CO and HCOOH production rates for poly-Cu in the same potential range. In the Tafel plots (Fig. 2(c) and (d)), the anodized Cu electrode shows a slope of 176 and 149 mV dec^{-1} for CO and HCOOH production, respectively, which are lower than those of the poly-Cu (236 and 175 mV dec^{-1}). Moreover, a higher Tafel slope of 331 mV dec^{-1} for H_2 evolution was observed on anodized Cu electrode as compared to poly-Cu (260 mV dec^{-1}). These observations indicate that the anodized Cu surfaces is more favorable for the formation of the $CO_2^{\bullet-}$ intermediate at less negative applied potentials while suppressing H_2O reduction, resulting in an enhanced activity and selectivity for the CO_2 reduction [9,10].

To further evaluate the effects of the changes in surface structures on the catalytic properties, the electrosorption of oxygenated species (*e.g.,* O and/or OH) on anodized Cu surfaces was investigated to identify the exposed facets (Figs. 3 (a) and S8). The CV curve of poly-Cu is featureless due to its extremely low ECSA. In contrast, all the anodized Cu electrodes show three oxidation peaks that can be assigned to the electrosorption features of oxygenated species on low-index facets of *fcc* Cu [14,17]. Moreover, the peak intensity enhancement for the (1 0 0) and (1 1 1) facets is even more pronounced in comparison to that of the (1 1 0) facet (Fig. 3(a)). Consistent with the literature results [7], these observations clearly suggest that the enhanced activity and selectivity of the anodized Cu

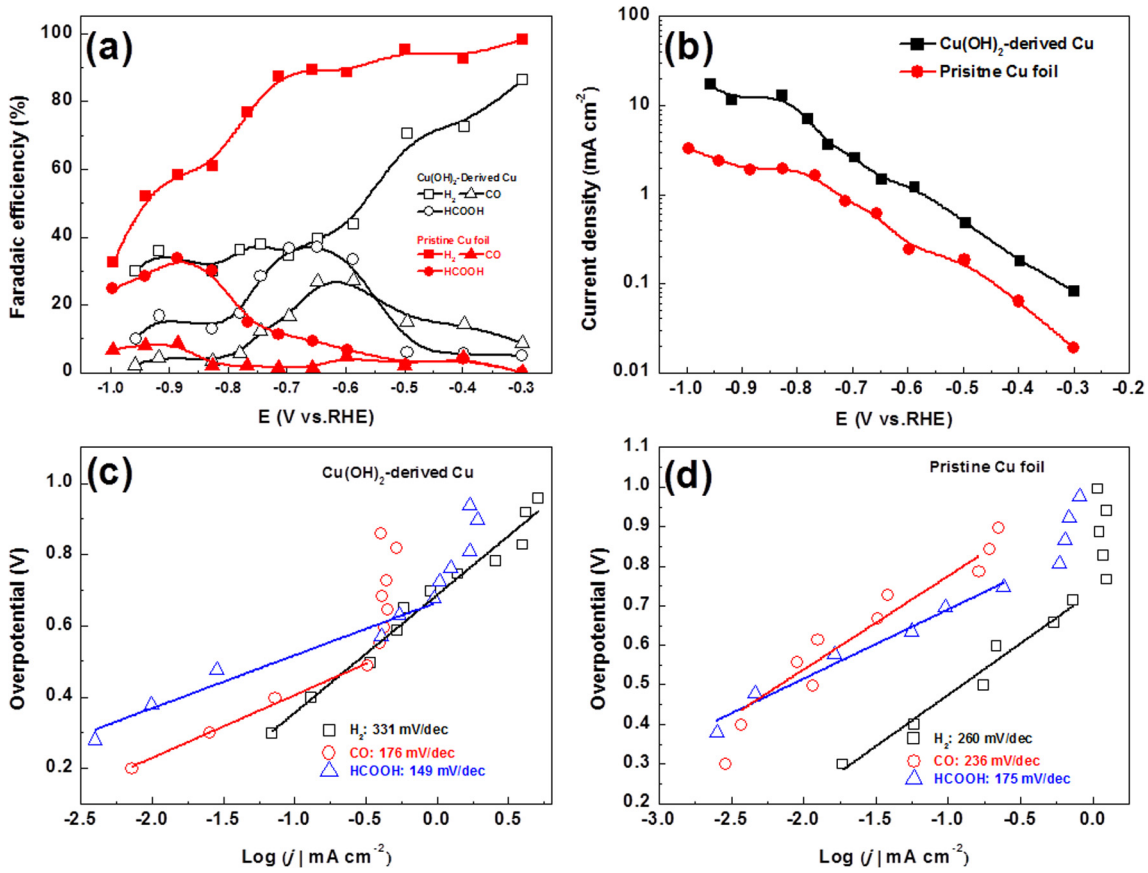

Fig. 2 (a) FEs for H_2, CO and HCOOH *vs.* applied potential in bulk electrolysis (with experimental errors of 5–10%). (b) Total current density *vs.* applied potential. (c, d) H_2, CO, and HCOOH Tafel plots.

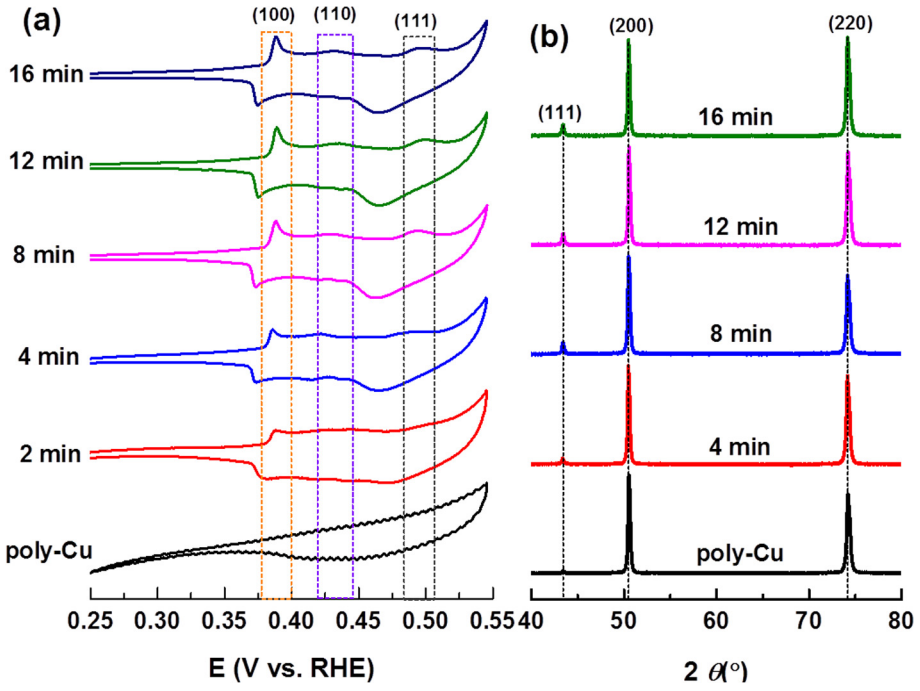

Fig. 3 (a) CVs of the poly-Cu and the anodized Cu electrodes after electroreduction at −0.64 V *vs.* RHE. The CVs were recorded in 1 M KOH with a scan rate of 20 mV/s. (b) Normalized XRD patterns of anodized Cu electrodes.

for the CO_2 reduction to CO and HCOOH are associated with the formation of more low-index Cu facets, especially (1 0 0) and (1 1 1). More (1 1 1) facets are favorable for the production of HCOOH at a lower overpotential, in agreement with the results that the HCOOH FE increases with the increasing amount of the (1 1 1) facet [7]. Moreover, all the anodized Cu electrodes show an enhanced peak intensity for the (1 1 1) facet (Fig. 3(b)), as compared to poly-Cu. Moreover, the intensity ratios of (1 1 1) to (2 0 0) for anodized Cu electrodes were plotted as a function of the HCOOH FE (Fig. S9). The HCOOH FE shows a positive correlation with the peak intensity ratio of (1 1 1) to (2 0 0). We thus attribute the improved HCOOH FE of the anodized Cu electrodes to the selectively preserved (1 1 1) surface during the anodization-reduction process.

4. Conclusion

A high surface area Cu electrode was prepared by a facile anodization-reduction process. An optimized anodized Cu electrode exhibited a lower onset potential and a 27% CO FE and 37% HCOOH FE at −0.64 V *vs.* RHE for the CO_2 reduction. The enhanced performance of the anodized Cu towards CO_2 reduction can be attributed to the high electrochemically active surface areas and the favorable formation of low-index Cu facets such as (1 0 0) and (1 1 1) facets. We have demonstrated that exploring the metal redox electrochemistry is a promising strategy and potentially useful for the preparation of highly efficient metal electrocatalysts for the low overpotential CO_2 reduction.

Acknowledgments

This work was supported by the King Abdullah University of Science and Technology (KAUST) and the National Natural Science Foundation of China (grant no. 21463001).

Appendix A. Supplementary data

Supplementary data associated with this article can be found, in the online version, at http://dx.doi.org/10.1016/j.jscs.2017.03.003.

References

[1] J. Qiao, Y. Liu, F. Hong, J. Zhang, Chem. Soc. Rev. 43 (2014) 631–675.
[2] M. Gattrell, N. Gupta, A. Co, J. Electroanal. Chem. 594 (2006) 1–19.
[3] A.A. Peterson, F. Abild-Pedersen, F. Studt, J. Rossmeisl, J.K. Nørskov, Energy Environ. Sci. 3 (2010) 1311–1315.
[4] P. Kuhl, E.R. Cave, D.N. Abram, T.F. Jaramillo, Energy Environ. Sci. 5 (2012) 7050–7059.
[5] S. Sen, D. Liu, G.T.R. Palmore, ACS Catal. 4 (2014) 3091–3095.
[6] R. Reske, H. Mistry, F. Behafarid, B. Roldan Cuenya, P. Strasser, J. Am. Chem. Soc. 136 (2014) 6978–6986.
[7] W.J. Durand, A.A. Peterson, F. Studt, F. Abild-Pedersen, J.K. Nørskov, Surf. Sci. 605 (2011) 1354–1359.
[8] D. Kim, J. Resasco, Y. Yu, A.M. Asiri, P.D. Yang, Nat. Commun. 5 (2014) 4948.
[9] C.W. Li, M.W. Kanan, J. Am. Chem. Soc. 134 (2012) 7231–7234.
[10] D. Raciti, K.J. Livi, C. Wang, Nano Lett. 15 (2015) 6829–6835.
[11] Y.-C. Hsieh, S.D. Senanayake, Y. Zhang, W. Xu, D.E. Polyansky, ACS Catal. 5 (2015) 5349–5356.
[12] L.Q. Zhou, C. Ling, M. Jones, H.F. Jia, Chem. Commun. 51 (2015) 17704–17707.
[13] J.M.M. Droog, C.A. Alderliesten, P.T. Alderliesten, G.A. Bootsma, J. Electroanal. Chem. 111 (1980) 61–70.
[14] J.M.M. Droog, B. Schlenter, J. Electroanal. Chem. 112 (1980) 387–390.
[15] M.C. Biesinger, L.W.M. Lau, A.R. Gerson, R.St.C. Smart, Appl. Surf. Sci. 257 (2010) 887–889.
[16] M. Ma, K. Djanashvili, W.A. Smith, Angew. Chem. Int. Ed. 55 (2016) 6680–6684.
[17] S. Min, X. Yang, A.-Y. Lu, C.-C. Tseng, M.N. Hedhili, L.-J. Li, K.-W. Huang, Nano Energy 27 (2016) 121–129.